Numerically controlled 8-channel IQ-transmitter with programmable synchronous carrier settings

Chris Stevens, Xavier Vanhoutte and Wim Vantomme - Technical University Kortrijk
Hendrik Rogier, senior member IEEE and Daniel De Zutter, Fellow IEEE - Ghent University

Abstract **— This paper describes the design, implementation and validation of a low-cost synchronous and phase coherent IF-front-end as part of a 8x8 IQ-MIMO wireless transmit system for wireless applications in the 2.4-2.5 GHz ISM band. The precision IF-front-end is designed to be used as a first up-conversion block from baseband to IF (intermediate frequency). The second up-conversion from IF to RF is accomplished by an RF-front end (beyond the scope of this paper). It also serves as a wireless testbed for smart antenna and MIMO transmission. The proposed 8-channel IF-front-end features the important property that it is possible to perfectly synchronize the eight carrier signals in time, phase and frequency. Moreover, each of the eight carrier signals can operate at a different but fixed frequency and different but constant phase, allowing to fix any frequency difference (32 bit resolution) and phase difference (16 bit resolution) between the 8 channels. Extreme care was also taken among the synchronization between the different channels in the RF-paths of the whole system.**

Index Terms **— MIMO systems, RF-design, transmitters, wireless communication**

I. Introduction

THE functional block diagram of the proposed IF-front-end of the MIMO transmitter is shown in Fig. I.1. The IF-stage performs an up-conversion of eight sampled IQ-signals (16-bit resolution) to an IF-frequency. The data samples of the eight baseband I and Q signals are first interpolated by an interpolation filter, then complex modulated in QAM (quadrature amplitude modulation) to an intermediate frequency (IF) and sent to two digital-to-analog converters as two complex QAM signals. Finally, the analog outputs of the DACs are sent to calibration circuits allowing low pass filtering (LPF) and precision gain calibration of the IQ-channels (GC). Each IQ-channel can be fixed at any IF-frequency (32 bit resolution) and any phase (16 bit resolution) controlled by a numerical oscillator (NCO). The synchronous central clocks for the eight IQ-channels are delivered to the output DACs by the clock generation board, a carefully designed PLL-system around the Texas Instrument's CDCM7005 clock synchronizer chip [1], [2].

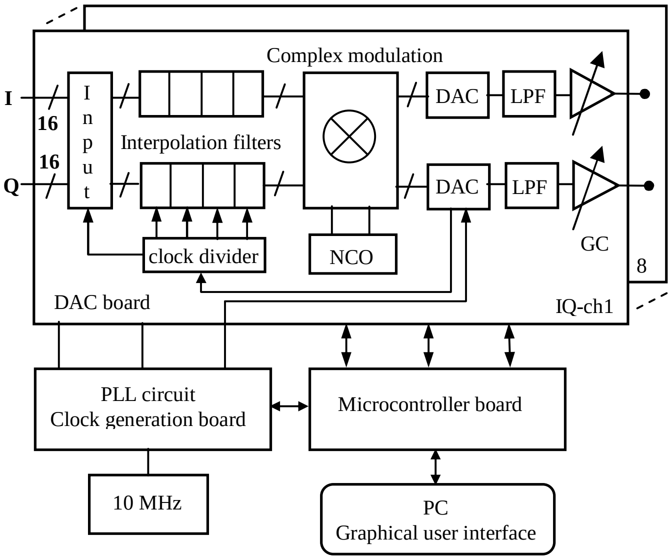

Fig. I.1. Functional block diagram of transmitter

The IF-block is controlled by means of a graphical user interface (GUI), allowing the user to set all the system parameters in a user-friendly way (see Fig. I.2). An intelligent interface board receives the data from the GUI and sends them to the hardware boards. Data from the boards is read by the interface and written to the GUI for further manipulation. The microcontroller board is build around the PIC18LF4550 microcontroller from Microchip [3].

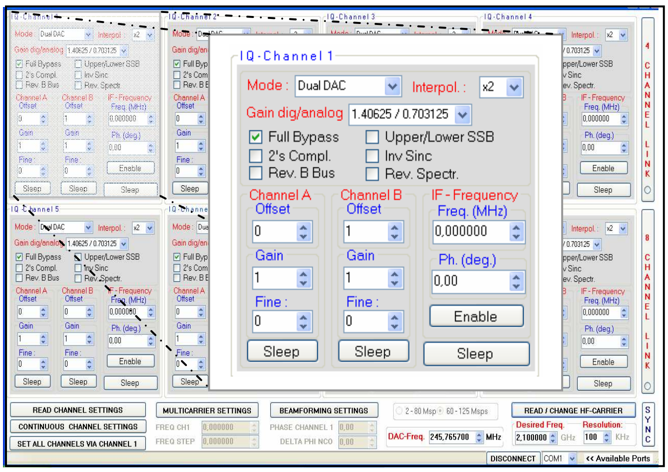

Fig. I.2. Graphical user interface

C. Stevens, X. Vanhoutte and W. Vantomme are with the Electronic Engineering Department, Technical University Kortrijk, Kortrijk, Belgium (phone:+32-56-241211;fax:+32-56-241224;e-mail:chris.stevens@howest.be).
H. Rogier and D. De Zutter are with the Department of Information Technology, Ghent University, Ghent, Belgium (e-mail: hendrik.rogier@ugent.be)

II. DESCRIPTION OF THE IF-FRONT-END

A. Block diagram

The IF-part of the MIMO-system is built around eight DAC5686 integrated circuits from Texas Instruments [4]. Fig. II.1 shows the simplified block diagram of one DAC5686.

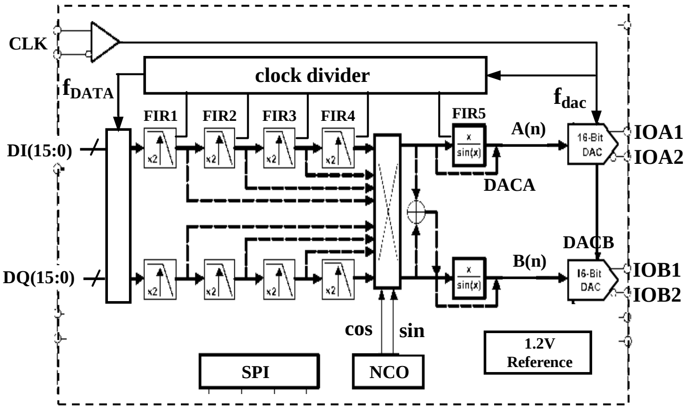

Fig. II.1. Block diagram of DAC5686

The DAC5686 contains two 16-bit high-speed digital-to-analog converters (DACA and DACB) with integrated 2x, 4x, 8x and 16x interpolation filters, a numerically controlled oscillator (NCO), an on-board clock divider, and on-chip voltage reference. The two CMOS DACs at the output of each DAC5686 have a differential output that consists of segmented arrays of NMOS current sinks, capable of sinking a full-scale output current I_{FS} up to 20 mA. Differential current switches direct the current of each current source through either one of the complementary output nodes (IOA1,IOA2 for DACA and IOB1,IOB2 for DACB). So, the complementary output currents enable differential operation, and thus cancelling out common mode noise sources (digital feed-through, on-chip and PCB noise), dc offsets and even order distortion components. The full-scale output current I_{FS} for both DACs is set using external bias resistors in combination with the on-chip bandgap voltage reference source (+1.2 V) and can be adjusted from 2mA to 20mA.

The 16-bit samples DI(15:0) and DQ(15:0) of the eight baseband I and Q signals are sent at a data rate f_{DATA} through two independent I and Q data paths consisting of four cascaded half-band interpolation filters (FIR1, FIR2, FIR3, FIR4). This interpolating filtering increases the DAC update rate, thereby enabling relaxed analog post-filtering. The interpolation factor L can be selected as 2x, 4x, 8x, or 16x. After interpolation a complex mixing operation is performed followed by an optional inverse sinc filter (FIR5) reducing sinx/x roll off. Finally the complex mixing signals are fed to the digital-to-analog converters converting the digital mixing signals to analog signals at a DAC rate f_{dac} (generated by the clock generation board). Depending on the selected interpolation factor L the DAC-clocks are internally divided to the appropriate clock signals for the interpolation filters. There is a fixed relationship between the input data rate f_{DATA} at which the input samples are read and the DAC rate f_{dac} at which the samples are written out :

$$f_{DATA} = \frac{f_{dac}}{L} \tag{1}$$

If the IF-front-end is preceded by an AD-converter block and the data clock (f_{DATA}) is used as the sample clock, then to avoid aliasing the input bandwidth is restricted to :

$$BW = \frac{f_{DATA}}{2} = \frac{f_{dac}}{2L} \tag{2}$$

The DAC5686's mixing frequencies and phases are flexibly chosen with the programmable NCO. The NCO produces two quadrature carrier signals $\cos(\omega_c nT+\theta_c)$ and $\sin(\omega_c nT+\theta_c)$ where $T=1/f_{dac}$. The frequency ω_c and phase θ_c of the carrier signals are given by

$$\begin{aligned} \omega_C &= x\frac{\omega_{dac}}{2^{32}} \quad ; \quad 0 < x < 2^{32} \quad \text{(32 bit resolution)} \\ \theta_C &= x\frac{\pi}{2^{15}} \quad ; \quad 0 < x < 2^{16} \quad \text{(16 bit resolution)} \end{aligned} \tag{3}$$

B. Output configuration

For practical applications the DAC outputs are loaded with a resistive load R_L as can be seen in Fig. II.2.

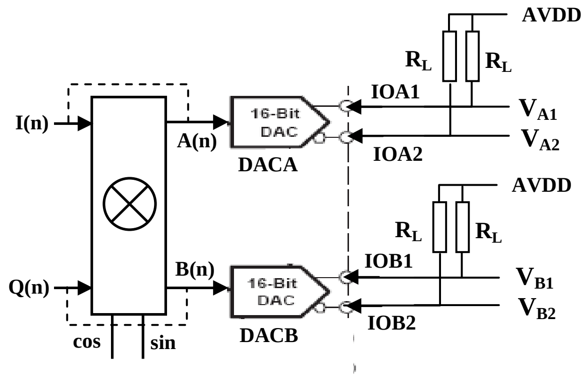

Fig. II.2. Output configuration for one IQ-channel

The DAC5686 can accept and process input data in full binary or two's complement format. Let I(n), Q(n) be the decimal representations of the baseband I- and Q-samples after interpolation and A(n), B(n) the decimal representations of the input samples of the DACs after complex mixing ($0 <$ A(n), B(n), I(n), Q(n) $< 2^{16}-1$ for full binary format and $-2^{15} <$ A(n), B(n), I(n), Q(n) $< 2^{15}-1$ for two's complement format). The complementary output currents can be expressed as

$$\begin{aligned} IOA1 &= mI_{FS} - I_{FS}\frac{A(n)}{2^{16}} \quad ; \quad IOA2 = (1-m)I_{FS} + I_{FS}\frac{A(n)}{2^{16}} \\ IOB1 &= mI_{FS} - I_{FS}\frac{B(n)}{2^{16}} \quad ; \quad IOB2 = (1-m)I_{FS} + I_{FS}\frac{B(n)}{2^{16}} \end{aligned} \tag{4}$$

where m=1 for full binary mode and m=1/2 for two's complement mode.

C. Modes of operation

For each IQ-channel the IF-front-end provides three modes of operation selectable by the user via the GUI : dual-channel mode, single-sideband mode and quadrature modulation mode.

In ***dual-channel mode*** there is no complex mixing (NCOs off), so this mode can be used as a test mode for the interpolation filtering and the DA-conversion.

Single-sideband mode provides an alternative interface to analog quadrature RF-modulators allowing, after RF up-mixing, an upper (USB) or lower (LSB) single-sideband RF-signal (which will be the case in our whole MIMO-transmitter). In single-sideband mode the DAC5686 performs two complex QAM modulations, forming a Hilbert pair according to

$$\begin{aligned}A(n) &= C + \mathrm{Re}\left[(I'(n) \pm jQ'(n))e^{j(\omega_c nT+\theta_c)}\right]\\ &= C + I'(n)\cos(\omega_C nT+\theta_C) \mp Q'(n)\sin(\omega_C nT+\theta_C)\\ B(n) &= C \pm \mathrm{Im}\left[(I'(n) + jQ'(n))e^{j(\omega_c nT+\theta_c)}\right]\\ &= C \pm (Q'(n)\cos(\omega_C nT+\theta_C) + I'(n)\sin(\omega_C nT+\theta_C))\end{aligned} \tag{5}$$

where $C=2^{15}$, $I'(n)=I(n)-2^{15}$, $Q'(n)=Q(n)-2^{15}$ for full binary format and C=0, $I'(n)=I(n)$, $Q'(n)=Q(n)$ for two's complement format. The sign of the quadrature term in A(n) and the sign of B(n) can be selected by the user via the GUI. By substituting (5) in (4) for full binary (m=1) and two's compliment format (m=1/2) and taking into account that for example V_{A1}=AVDD-R_LIOA1, the output signals V_{A1},V_{A2},V_{B1} and V_{B2} in Fig. II.2 can be calculated. They are given by :

$$\begin{aligned}V_{A1} &= V_{DC} + \alpha[I'(n)\cos(\omega_C nT+\theta_C) \mp Q'(n)\sin(\omega_C nT+\theta_C)]\\ V_{A2} &= V_{DC} - \alpha[I'(n)\cos(\omega_C nT+\theta_C) \mp Q'(n)\sin(\omega_C nT+\theta_C)]\\ V_{B1} &= V_{DC} \pm \alpha[Q'(n)\cos(\omega_C nT+\theta_C) + I'(n)\sin(\omega_C nT+\theta_C)]\\ V_{B2} &= V_{DC} \mp \alpha[Q'(n)\cos(\omega_C nT+\theta_C) + I'(n)\sin(\omega_C nT+\theta_C)]\end{aligned} \tag{6}$$

where the DC-component V_{DC} and the gain factor α are given by :

$$V_{DC} = AVDD - \frac{R_L I_{FS}}{2} \quad ; \quad \alpha = \frac{R_L I_{FS}}{2^{16}} \tag{7}$$

In ***quadrature modulation mode***, DACA is switched off and DACB presents one of the two complex QAM modulations according to :

$$\begin{aligned}B(n) &= C + \mathrm{Re}\left[(I'(n) + jQ'(n))e^{j(\omega_c nT+\theta_c)}\right]\\ &= C + I'(n)\cos(\omega_C nT+\theta_C) - Q'(n)\sin(\omega_C nT+\theta_C)\end{aligned} \tag{8}$$

or

$$\begin{aligned}B(n) &= C + \mathrm{Im}\left[(I'(n) + jQ'(n))e^{j(\omega_c nT+\theta_c)}\right]\\ &= C + Q'(n)\cos(\omega_C nT+\theta_C) + I'(n)\sin(\omega_C nT+\theta_C)\end{aligned} \tag{9}$$

By substituting (8),(9) in (4) we obtain similar expressions as in single-sideband mode for the outputs V_{B1} and V_{B2} in Fig. II.2.

D. Lowpass filtering and precision gain calibration

One of the complementary outputs of each DAC is sent to a lowpass filtering and gain calibration circuit as illustrated in Fig. II.3 for one channel. The calibration circuits are built around fully differential TI-THS4503 amplifiers [5]. Fig. II.4 shows some simulations of the circuit.

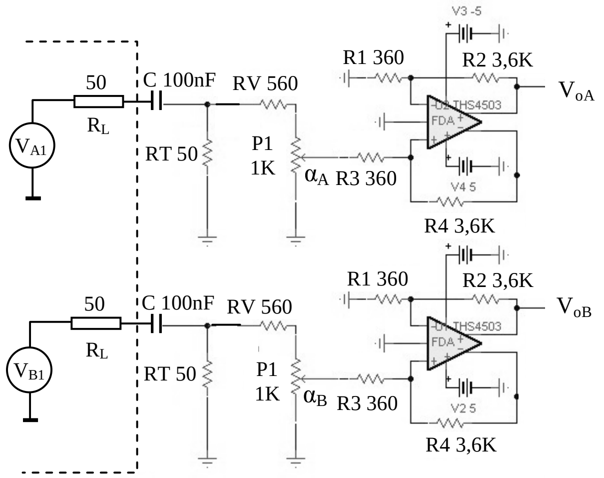

Fig. II.3. Lowpass filtering and gain calibration circuit

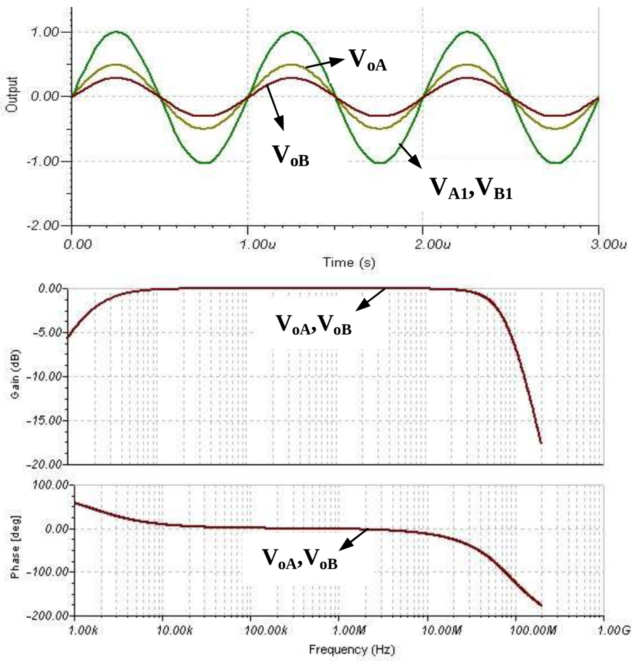

Fig. II.4. Time domain and frequency domain analysis

The sources V_{A1} and V_{B1} represent the output signals of the DACs if they are not loaded with the calibration circuit (open-terminal Thevenin voltages). They were calculated in section II.C ((6). R_L (50Ω) represents the Thevenin impedance as seen from the calibration circuits into the DACs. The DAC output signals are AC-coupled, canceling out the DC-components. The amplifier circuit has a 3-dB bandwidth of approximately 70 MHz and a gain G (controlled with the potentiometers P1) between 0 and 1 for input signals with 50Ω source impedance (between 0 and 2 for input signals with zero source impedance). Fig. II.4 shows a time domain analysis for a 50Ω-1V/1MHz input signal (potentiometers set to α_A=50%,α_B=25%) and a frequency domain analysis between 1kHz and 200MHz for a 50Ω-1V input signal (potentiometers set to α_A=α_B=100%)

III. Calibration and Applications

In Fig. III.1 a photograph of the realized IF-block illustrates our realization. The different parts are recognized : the power block, microcontroller circuit, clock generation board, DAC boards and gain calibration circuit.

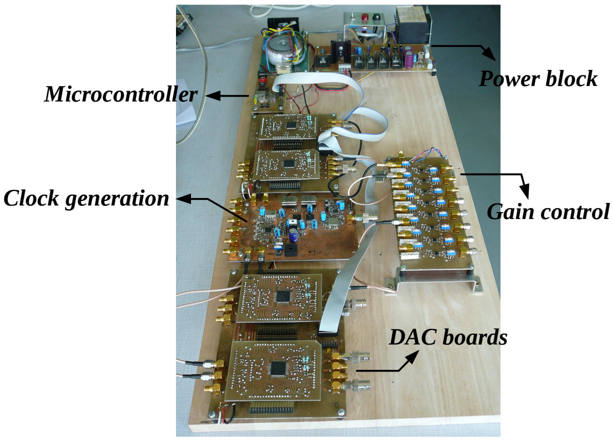

Fig. III.1. Photograph of the realized IF-block

Fig. III.2 gives a simple block model for the IF-front-end. Since the output samples of the DACs are converted into analog signals (by the lowpass and the gain calibration circuits) and the DC-components are cancelled out (by the input capacitors of the calibration circuits), we can obtain general expressions for the two output signals of each IQ-channel i (i=0,1,…,7) as a function of the discrete input samples ($I_i(n)$,$Q_i(n)$), the parameter settings (via the GUI) and the gain calibration.

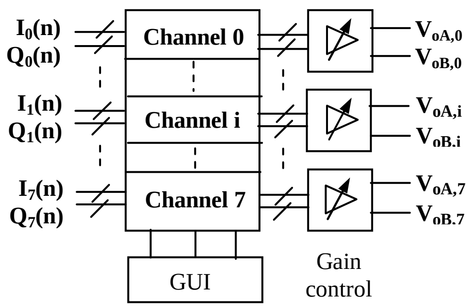

Fig. III.2. Simplified model of IF-front-end

Using (6),(7) the output signals of any IQ-channel in single-sideband mode are obtained by replacing the discrete samples $I_i'(n)$,$Q_i'(n)$ of each IQ-channel i with their analog counterparts $I_i'(t)$,$Q_i'(t)$ (similar expressions can be obtained for QAM mode). If the system accepts and processes data in two's complement format the two outputs of any IQ-channel are given by

$$\begin{aligned} V_{oA,i} &= A_i\left[I_i(t)\cos(\omega_{c,i}t+\theta_i) \mp Q_i(t)\sin(\omega_{c,i}t+\theta_i)\right] \\ V_{oB,i} &= (\pm)B_i\left[Q_i(t)\cos(\omega_{c,i}t+\theta_i) + I_i(t)\sin(\omega_{c,i}t+\theta_i)\right] \end{aligned} \quad (9)$$

$\omega_{c,i}$ and θ_i are the carrier frequency and phase of channel i. A_i and B_i are the gains and can be written as the product of a coarse gain $\alpha_{A,i}$ ($\alpha_{B,i}$) and a precision gain $G_{A,i}$ ($G_{B,i}$) :

$$\begin{aligned} &A_i = G_{A,i}\alpha_{A,i} \quad ; \quad B_i = G_{B,i}\alpha_{B,i} \\ &\alpha_{A,i} = (R_L I_{FSA,i})/2^{16}\,;\, \alpha_{B,i} = (R_L I_{FSA,i})/2^{16} \end{aligned} \quad (10)$$

where $I_{FSA,i}$ and $I_{FSB,i}$ are the full scale currents of DACA and DACB for channel i. The sign of the sine term in $V_{oA,i}$ and the sign of $V_{oB,i}$ are chosen by setting the reverse spectrum bit (Rev. Spectr.) and the Upper/Lower SSB-bit in the GUI. If the processing of the discrete samples is done in full binary format we have the same expression except that $I_i(t)$ and $Q_i(t)$ in (9) are replaced with ($I_i(t)$-2^{15}) and ($Q_i(t)$-2^{15}) respectively. The frequency (32-bit resolution) and phase (16-bit resolution) of any channel i are given by :

$$\begin{aligned} &0 < \omega_{c,i} < x\frac{\omega_{dac}}{2^{32}} \quad ; \quad 0 < x < 2^{32} \quad \text{(32 bit resolution)} \\ &0 < \theta_i < x\frac{\pi}{2^{15}} \quad ; \quad 0 < x < 2^{16} \quad \text{(16 bit resolution)} \end{aligned} \quad (11)$$

For calibration purposes, a coarse gain (α_{Ai} , $\alpha_{B,i}$) for each channel can be set by setting the full scale currents I_{FS} between 0 and 20mA via the GUI. The step size equals 20mA/16. A fine gain calibration for each channel can be obtained with the precision gain calibration circuits ($0<G_{A,i}$, $G_{B,i}<1$).

If the input samples of any channel are held constant then the system can be used as a precision multi-channel vari-phase generator with programmable amplitude, frequency and phase settings. When used as the IF-part of a complete MIMO-transmitter with RF-front-end, holding the input samples at a constant level allows the user to do a precision calibration of the complete MIMO-system as described above, thereby compensating for amplitude and phase mismatches in the RF-paths of the whole transmitter.

Many other applications are possible such as beam forming, transmit diversity, spatial multiplexing and synchronous multi-carrier generation. Transmit diversity and spatial multiplexing require synchronous carrier signals with same carrier frequency ω_c whereas beamforming requires, in addition, a fixed phase difference $\Delta\theta$ between adjacent channels, i.e.

$$\omega_{c,i} = \omega_c \;\forall i \quad ; \quad \theta_i = \theta_0 + (i\,\Delta\theta)$$

where θ_0 is the phase of the reference channel (channel 0). Multi-carrier generation on the other hand requires synchronous carrier signals with the same phase but with a fixed frequency difference between them :

$$\omega_{c,i} = \omega_{c,0} + i\Delta\omega_c \ \forall i \quad ; \quad \theta_i = \theta_0$$

where $\omega_{c,0}$ is the frequency of the reference channel (channel 0) and $\Delta\omega_c$ the frequency difference between adjacent channels. Our system was specifically designed to perform beam forming, transmit diversity, spatial multiplexing, as well as multi-carrier generation. For each application, the parameters are set in a user-friendly way via the GUI.

In the near future the proposed IF-block will be extended with an improved RF-board containing 8 RF QAM modulators as a second up-conversion from IF to RF as shown in Fig. III.3. The IF-block will then be used as the central programmable and calibration part of a complete RF MIMO transmitter for wireless applications in the 2.4-2.5 GHz ISM band. In single sideband mode our IF-block can for each IQ-channel generate two output signals that form a Hilbert pair. Using these two signals as the input signals of the RF QAM modulators results in an upper or lower single sideband signal in the RF domain without mirror components, thus without the need for supplementary rejection filters (as is the case in most double up-conversion systems).

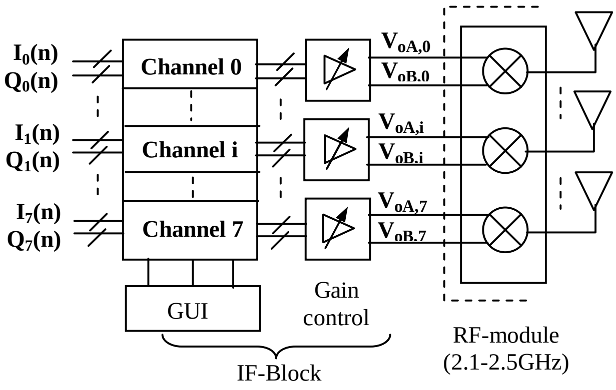

Fig. III.3 RF-MIMO-transmitter

IV. Measurements

Some oscilloscope images of measurements on the IF front-end are shown in Fig. IV.1. The figure illustrates some steps in the phase matching calibration of two different IQ-channels: before (a), during (b) and after phase matching (c)

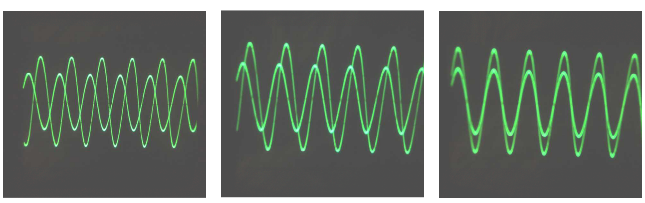

(a) before phase matching (b) during phase matching (c) after phase matching

Fig. IV.1. Phase matching calibration

V. Contributions

We want to thank some colleagues for the contributions they made during the design and development of the proposed IF-front-end. An important part of the whole system is the graphical user interface (although not explained in detail in this paper). Here we want to thank F. De Pauw, S. Verstockt, and H. Ameel for their very useful advice, help, tips and tricks concerning the software development of the graphical user interface. Their experience with writing software for GUIs was a great help.

References

[1] Texas Instruments, “CDCM7 3.3-V HIGH PERFORMANCE CLOCK SYNCHRONIZER AND JITTER CLEANER”, scas793c-june 2005-revised December 2007.

[2] M. Cosaert, C. Stevens, “Study and implementation of a programmable HF-oscillator via PLL for QAM-modulation”, master thesis, 2006-2007, Dept. Electronics, HOWEST, Kortrijk, Belgium

[3] J. Dedecker, G. Vandelannoote, C. Stevens, “Design of a configurable QAM data link for the ISM band”, master thesis, 2006-2007, Dept. Electronics, HOWEST, Kortrijk, Belgium

[4] Texas Instruments, “DAC5686 16-BIT, 500-MSPS,2x-16x INTERPOLATING DUAL-CHANNEL DIGITAL-TO-ANALOG CONVERTER”, slws147e-april 2003-revised June.

[5] Texas Instruments, “THS4502, THS4503 LOW DISTORSION FULLY DIFFERENTIAL AMPLIFIERS”, slos3520-april 2003-revised January 2004.

Chris Stevens received the master degree in Electronic Engineering from the Ghent University, Ghent, Belgium in 1980. In 1983 he joined the Technical University Kortrijk where he is now a full professor at the department Electronics. His teaching activities are in the domains of HF-electronics, signal processing, communications systems and micro-electronics. Beyond his teaching activities he is engaged in research and development of HF- and wireless communications systems in cooperation with the department Information Technology (INTEC) of the Ghent University and within the Association Research Group “Network Topologies and Distributed Software”.
E-mail: chris.stevens@howest.be

Xavier Vanhoutte graduated in electronics at the Technical Institute, department Electronics, Kortrijk, Belgium in 1977. Since then he is with the Technical University Kortrijk where he is a technical collaborator at the department Electronics within the telecommunications laboratory. His activities are in the domains of analog and HF-electronics. He is also involved in the research activities on HF- and wireless communications systems at the department. Since several years he is a radio-amateur.
E-mail: xavier.vanhoutte@howest.be

Wim Vantomme received the master degree in industrial science at the Technical University Kortrijk in 2005. At the moment he’s doing Ph.D. research in the field of RF instrumentation and application.
E-mail: wim.vantomme@howest.be

Hendrik Rogier
Hendrik Rogier (M. Sc. 1994, Ph.D. 1999, Ghent University) is now an associate professor of Electromagnetics at the Engineering Faculty of Ghent University. He received the URSI Young Scientist Award at the 2001 URSI Symposium on Electromagnetic Theory and at the 2002 URSI General Assembly, and is a Senior Member of the IEEE. He published more than 45 journal publications. His current research interests are the analysis of electromagnetic waveguides, electromagnetic simulation techniques applied to EMC and signal integrity problems, as well as to indoor propagation and antenna design, and smart antenna systems for wireless networks.
E-mail: hendrik.rogier@ugent.be

Daniel De Zutter
Daniël De Zutter (M. Sc. 1976, Ph.D. 1981, Habilitation 1984, Ghent University) is now a full professor of Electromagnetics at the Engineering Faculty of Ghent University. In 2000 he was elected as Fellow of the IEEE. He published more than 150 journal publications. In the past 4 years he served as dean of the faculty.
E-mail: daniel.dezutter@ugent.be